as part of the 'background' and would be deducted from the total scattered intensity (Fig. 1).

For cubic crystals, the effect of neglecting thermal diffuse scattering contributions to the integrated intensities results in a systematic error, increasing in magnitude with diffraction angle. The overall result is to decrease appreciably the Debye–Waller temperature factors (*e.g.* Al ~ 11%; KCl ~ 15%, for the examples given in Table 1).

Although the Mössbauer measurements may be subject to some uncertainty, the reasonable agreement obtained with the predicted values for Al and KCl would appear to make further such measurements worthwhile.

The author gratefully acknowledges the help of Dr E. G. Steward for valuable discussion and kindly interest during the progress of this work.

APPENDIX

Approximate relationships to calculate $\langle K[ABC]_{hkl}\rangle$ for cubic crystals

(i) A direct method for calculating an approximate value for $\langle K[ABC]_{hkl}\rangle$ is to find the arithmetic mean, with appropriate weighting, for values of $K[ABC]_{hkl}$ over the $\langle 100\rangle$, $\langle 110\rangle$, and $\langle 111\rangle$ directions, which results in the expression:

$$\langle K[ABC]_{hkl}\rangle_{\text{approx}} = 1/13\,.\,(s_1+4(s_2+s_3+s_4+s_5)+8s_6)\,.$$

$s_1=1/c_{11}$, $s_2=1/c_{44}$, $s_3=1/(c_{11}-c_{12})$, $s_4=1/(c_{11}+c_{12}+2c_{44})$, $s_5=1/(c_{11}+2c_{12}+4c_{44})$, $s_6=1/(c_{11}-c_{12}+c_{44})$ (Ramachandran & Wooster, 1951).

(ii) Nilsson (1957) has also approximated a quantity, $\bar{\kappa}$, (it can readily be shown that $K[ABC]_{hkl}=\frac{1}{3}\,.\,\kappa$) and suggested the expression:

$$\bar{\kappa}_{\text{approx}}=\frac{\frac{1}{5}\,.\,b_1(c_{11}+c_{12})+c_{44}(2c_{11}+c_{44})}{1/105\,.\,b_1^2b_2+\frac{1}{5}\,.\,(c_{11}+c_{12})c_{44}+c_{11}c_{44}^2}\,,$$

where

$$b_1=c_{11}-c_{12}-2c_{44}\,,\;\; b_2=c_{11}+2c_{12}+c_{44}\,.$$

Both methods of approximation are compared in Table 2 with the more exact evaluation of Nilsson (1957).

References

Butt, N. M. & O'Connor, D. A. (1967). *Proc. Phys. Soc.* **90**, 247.
Chipman, D. R. & Paskin, A. (1959). *J. Appl. Phys.* **30**, 1992, 1998.
Cochran, W. (1963). *Rep. Progr. Phys.* **26**, 1.
Cochran, W. & Pawley, G. S. (1964). *Proc. Roy. Soc.* A**280**, 1.
Cooper, M. J. & Rouse, K. D. (1968). *Acta Cryst.* A**24**, 405.
James, R. W. (1962). *The Optical Principles of the Diffraction of X-rays.* London: Bell.
Kamm, G. N. & Alers, G. A. (1964). *J. Appl. Phys.* **35**, 327.
Laval, J. (1939). Thesis, Paris.
Lonsdale, K. (1942). *Proc. Phys. Soc.* **54**, 314.
Lucas, B. W. (1968). *Acta Cryst.* A**24**, 336.
Nilsson, N. (1957). *Ark. Fys.* **12**, 247.
Norwood, M. H. & Briscoe, C. V. (1958). *Phys. Rev.* **112**, 45.
O'Connor, D. A. & Butt, N. M. (1963). *Phys. Letters*, **7**, 233.
Prasad, S. C. & Wooster, W. A. (1956). *Acta Cryst.* **9**, 38.
Ramachandran, G. N. & Wooster, W. A. (1951). *Acta Cryst.* **4**, 335, 431.
Schwartz, L. H. (1964). *Acta Cryst.* **17**, 1614.
Warren, B. E. (1953). *Acta Cryst.* **6**, 803.
Wooster, W. A. (1962). *Diffuse X-ray Reflexions from Crystals.* London: Oxford Univ. Press.

Acta Cryst. (1969). A**25**, 631

Thermal Etching of Dislocations in Zinc Crystallites Grown from the Vapour

By Ram Bilas Sharma*

Applied Sciences Department, Punjab Engineering College, Chandigarh, India

(*Received* 9 *October* 1968 *and in revised form* 22 *January* 1969)

Small single crystals of zinc of 99·99% purity were grown from the vapour at a temperature slightly less than the melting point. The dislocation structure of these crystallites was studied by thermal etching, which occurs when the crystals are cooled from the growth temperature to 10 to 15 °C below the melting point in a few minutes. Various types of etch figures were observed and the mechanisms of their formation are discussed. It seems, on the basis of the available evidence, that the etch figures correspond to dislocations.

Introduction

It is known that thermal etching can be applied to reveal dislocations in crystals of a number of metals and alloys, with the important exceptions of Zn, Cd, Mg and their alloys, which have a high vapour pressure at high temperatures.

It is shown here for the first time that thermal etching can also be applied to reveal dislocations in zinc crystals if the conditions of high vacuum and low undersaturation of vapour are obtained. The latter condition

---

* Present address: Physics Department, Shyam Lal College, Delhi University, Shahdara, Delhi-32, India.

was obtained in the present case by having an airtight enclosure where there was a large amount of back flux recondensing on the evaporating surfaces.

Experimental

Fine crystallites of zinc of 99·99% purity were grown from the vapour during the process of growth of zinc oxide whiskers.

A small quantity of zinc was heated up to a temperature of about 850°C when a large portion of it was transformed into zinc oxide vapour which enveloped the remaining metallic charge with a thick amorphous coating and then condensed in various crystalline forms, including whiskers. The coating of amorphous zinc oxide assumed the shape of a dome and finally, as a result of deposition in one direction resulting from the presence of a temperature gradient, that of a hollow beak with a closed end, covered on both the inside and outside with zinc oxide whiskers. This hollow beak acted as a fully airtight enclosure for the metal and its vapour. Whatever quantity of air remained in the enclosure was completely used up in oxidizing only a part of the vapour, thus causing a self-created vacuum for the remaining vapour; the vapour condensed in the form of fine unoxidized crystallites when the furnace was cooled to a few degrees below the melting point for zinc.

Thermal etching of the unoxidized crystallites occurred spontaneously when the specimens were cooled in a matter of minutes from the growth temperature to 10 to 15°C below the melting point.

Results and discussion

The growth of the crystallites takes place by condensation of vapour at a temperature slightly below the melting point of zinc. The surfaces of the crystallites are so smooth and shiny that further polishing treatment is not required before studying the surface features of as-grown specimens. Dislocations that are introduced in the crystals during growth and, further, during cooling in the high temperature range when thermal stresses are very high give rise to the formation of pits on the surface when thermal etching occurs.

The pits at the dislocations assume various shapes depending on a number of factors such as the surface orientation of the crystal, the position of the dislocation and the presence of an impurity atmosphere around the dislocation. The effect of surface orientation on the pit shape is illustrated in Figs. 1 and 2; the hexagonal pits of Fig. 1 are on the (0001) plane and the oval shaped pits of Fig. 2 are on an inclined plane. The density of dislocations intersecting the (0001) surface, as estimated by the etch-pit count, is found to be about 10^6 cm^{-2}.

Fig. 3 shows a large flat-bottomed pit; all other pits in the Figure are sharp-bottomed. The formation of the flat-bottomed pit indicates that the dislocation has moved away while the etching was still in progress. An interesting phenomenon depicted in Fig. 3 is the characteristic star shape shown by outer terraces of the pits which suggests that etching is not uniform but greater in certain directions. The star shape of the outer terraces of (0001) pits has been observed by George (1959) in vapour grown zinc crystals after chemical etching.

Fig. 4 shows the formation of a double pit – an outer primary pit with star-type terraces and an inner secondary pit of hexagonal shape containing the dislocation emergence point at its centre. The secondary pit is slightly removed from the centre of the primary pit.

The etch pattern of Fig. 4 is formed as a result of the presence of a jog or kink in the dislocation. The rate of attack of the etch, normal to the surface, is reduced when the kink is reached. This results in the slight shift of the secondary pit away from the centre of the primary pit. Such a phenomenon has been reported and discussed in greater detail by Ellis (1955) in the case of germanium, where the inner and lower terraces are concentric with the central depression while the outer ones are not.

The formation of etch grooves at dislocations is also observed with the help of thermal etching. These grooves are shown in Fig. 5. The average length of the grooves is about 7·7 microns and the density of these grooves is of the order of 10^6 cm^{-2}, which is the same as the density of pits on other crystal surfaces.

Further, it is noticed that some of the pits resulting from thermal etching have a spiral configuration. The size of such pits is very small and they are probably formed at screw dislocations.

It has been possible in the present case to reveal with the help of thermal etching not only individual dislocations, but grain boundaries too. Since the crystals were mostly single crystals, only sub-boundaries could be observed, in the form of small arrays of pits on crystal surfaces. Fig. 6 shows a sub-boundary originating from a highly stressed region, as suggested by a high concentration of etch pits there. In fact, at least two more sub-boundaries originate from this region of high stress, but they are only faintly visible in the photomicrograph. The average pit separation in the sub-boundary shown in Fig. 6 is about 2·3 microns.

Conclusions

The present investigations show that thermal etching of dislocations in zinc crystals is possible if the conditions of high vacuum and low undersaturation of vapour are satisfied and if the etching is carried out by cooling the crystals from the growth temperature – which is a few degrees below the melting point – to 10 to 15°C below the melting point, in a few minutes.

From the following observations, it seems that the etch pits and etch grooves observed have some correspondence to dislocations.

(1) The density of etch pits and etch grooves observed in the present investigations (10^6 cm^{-2}) is of the

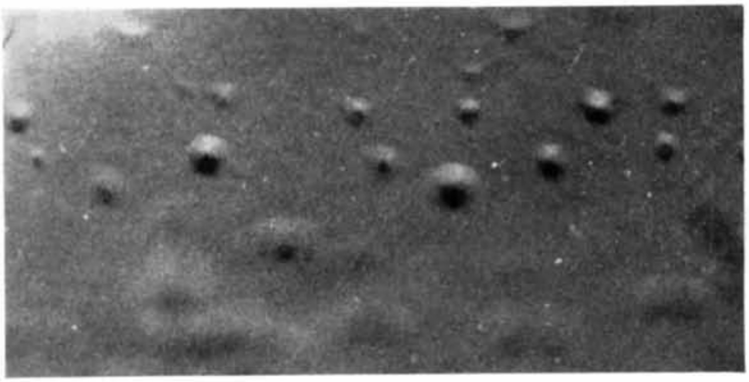

Fig. 1. Formation of hexagonal pits on an (0001) plane (1670*x*).

Fig. 2. Formation of oval shaped pits on a plane other than (0001) (1370 ×).

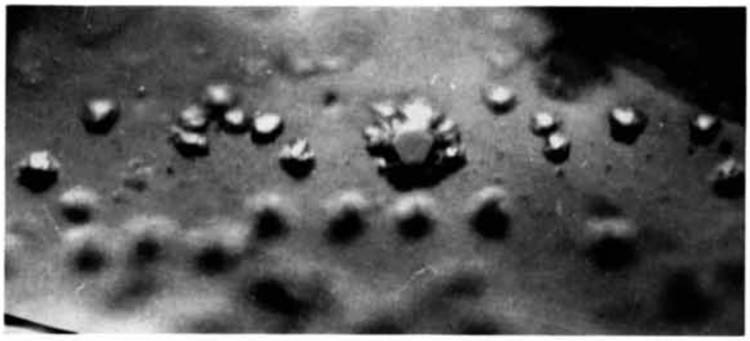

Fig. 3. A large flat-bottomed pit surrounded by small sharp-bottomed pits. The pits have star-type outer terraces (1010 ×).

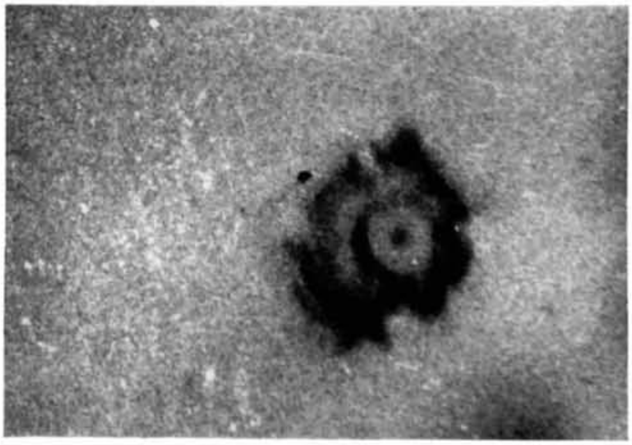

Fig. 4. Formation of a double pit. The inner secondary pit containing the dislocation emergence point at its centre is slightly displaced from the centre of the outer primary pit (3520 ×).

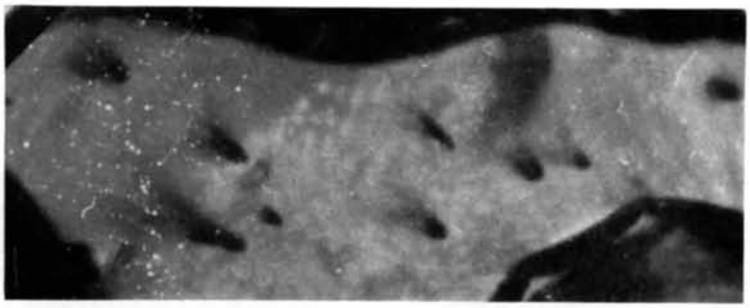

Fig. 5. Formation of etch grooves on a crystal surface (1970 ×).

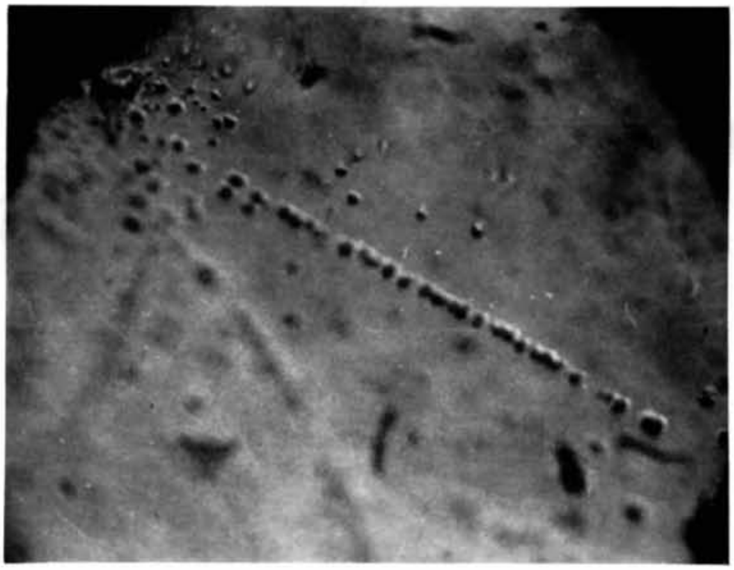

Fig. 6. A sub-boundary originating from a highly stressed region of the crystal surface (1090 ×).

same order as the expected density of dislocations in zinc single crystals grown under similar conditions.

(2) Besides individual etch pits, linear arrays of pits suggestive of small angle boundaries have been observed.

(3) The formation of a flat-bottomed pit, indicating that the dislocation has moved during etching, is noted.

The author is grateful to The Council of Scientific and Industrial Research, New Delhi, for providing research facilities and for awarding a research fellowship during the course of this work.

References

Ellis, S. G. (1955). *J. Appl. Phys.* **26**, 1140.
George, J. (1959). *Phil. Mag.* **4**, 1142.

Acta Cryst. (1969). A**25**, 633

Optical Activity in a Non-Enantiomorphous Crystal of Class $\bar{4}$: $CdGa_2S_4$

By M. V. Hobden

Royal Radar Establishment, Malvern, Worcestershire, England

(*Received* 22 *January* 1969)

Optical activity has been observed for the first time in a crystal of the non-enantiomorphous class $\bar{4}$. $CdGa_2S_4$ is optically isotropic at 4872 Å (20 °C) and this allows observation of optical rotation for propagation in directions away from the *c* axis. The magnitude of the optical rotatory power is 17·3 deg.mm^{-1} along ⟨100⟩ and 11·6 deg.mm^{-1} along ⟨110⟩. The form of the optical rotatory power for general directions in the (001) plane has the predicted symmetry, showing positive and negative lobes. The refractive indices and birefringence are temperature-dependent and the point of isotropy shifts from 4825 Å at 0 °C to 5780 Å at 400 °C.

Introduction

To a first approximation, light is propagated in crystalline media by two transverse linearly polarized modes of propagation. However, in media of certain symmetries a small perturbation to these linear modes can arise when the dimensions of the basic structure unit are not negligible compared with the wavelength of the light. In general the two modes of propagation are then elliptically polarized with slightly modified phase velocities. Optical phenomena due to these small perturbations are generically termed optical activity.

A phenomenological theory of optical activity, based upon a gyration tensor (Nye, 1964) has explained the symmetry properties of optical activity in the various crystal classes with success. It can be shown that optical activity is allowed by symmetry in only 15 of the 32 crystal classes. These are the 11 enantiomorphous classes 1, 2, 222, 4, 422, 3, 32, 6, 622, 432 and 23 and the four non-enantiomorphous classes *m*, *mm*2, $\bar{4}$ and $\bar{4}2m$. It has recently been shown for the first time that optical activity can exist in a non-enantiomorphous crystal (Hobden, 1967, 1968*a*); it was found that $AgGaS_2$ (class $\bar{4}2m$) was accidently optically isotropic at 4974 Å and this allowed the optical rotatory power to be measured in directions away from the *c* axis.

$CdGa_2S_4$ (class $\bar{4}$) has a similar isotropy point and also exhibits optical activity (Hobden, 1968*b*). This phenomenon has been examined in more detail and the dependence of the optical rotatory power on direction of propagation and also crystal temperature is now reported.

The structure of $CdGa_2S_4$

It has been shown by Hahn, Frank, Klingler, Storger & Storger (1955), using powder diffraction techniques, that $CdGa_2S_4$ has spatial symmetry $I\bar{4}$ with cadmium on the (*a*) sites, gallium on the (*b*) and (*c*) sites, and sulphur on the (*g*) sites ($x=0{\cdot}27$, $y=0{\cdot}26$, $z=0{\cdot}14$). It is therefore a uniaxial, acentric non-enantiomorphous crystal of class $\bar{4}$.

The compound was prepared by fusion of CdS and Ga_2S_3, each of which was prepared from high purity elements. Slow crystallization by the Stockbarger technique (m.p. ~ 1050 °C) in sealed quartz tubes produced a polycrystalline matrix from which single-crystal pieces up to 8 mm in diameter were cut. Polished plates prepared from these crystals were examined with the polarizing microscope and found to be yellow in colour, uniaxial, and of good optical quality. These plates gave a positive response to the Giebe–Scheibe test for piezoelectricity thereby confirming acentricity. X-ray powder patterns agreed closely with a computed pattern based upon the reported structure, though our unit-cell dimensions were $a=5.54(6)$ and $c=10{\cdot}16$ Å ($K\alpha_1=1{\cdot}5405$ Å) compared with $a=5{\cdot}57(6)$ and $c=10{\cdot}08$ Å derived from the published data mentioned above. The measured density of the polycrystalline matrix, which